GPS Solutions (2027) 31:4
https://doi.org/10.1007/s10291-026-02168-9

RESEARCH

Hardware-in-the-loop verification of GNSS-based orbit determination, time synchronization, and oscillator disciplining for LEO-PNT

F. Kunzi[1] · J. Holtkamp[1] · O. Montenbruck[1]

Received: 23 June 2026 / Accepted: 11 October 2026
© The Author(s) 2026

Abstract
Positioning, navigation and timing (PNT) services from low Earth orbit (LEO) present an important alternative or complement to established global satellite navigation systems (GNSSs). Within a LEO-PNT system, proper knowledge of the instantaneous LEO satellite position and onboard time is essential for the generation of navigation signals. Among the currently proposed LEO-PNT systems, GNSS-based onboard orbit determination and time synchronization (ODTS) is a widely considered concept for the autonomous generation of navigation signals and satellite ephemerides. To demonstrate the feasibility of autonomous real-time ODTS and assess the achievable performance, a realistic hardware-in-the-loop simulation for a LEO environment is employed. As a device under test, a miniature satellite payload developed for the ATOMIC (Autonomous Time and Orbit Determination for Micro-satellite Constellations) experiment is utilized, which involves a multi-constellation GNSS receiver, a chip-scale atomic clock (CSAC) and a micro-processor executing the GNSS-based real-time orbit determination and clock disciplining process. For maximum realism, the simulation replicates the real-world orbital dynamics of a representative LEO satellite at 1336 km altitude along with the true GPS and Galileo orbits and clocks as well as the actual broadcast navigation messages transmitted by those constellations on the day of interest. The results for a 24 h data arc show that a 3D root mean square (RMS) position error of 9.5 cm can be achieved, while the clock phase of the onboard oscillator can be synchronized to the GNSS system time scale with a precision of 1.0 ns. While the carrier-phase-based real-time ODTS enables a significantly better clock synchronization than traditional GNSS-disciplined oscillators, the achieved performance is ultimately limited by the broadcast ephemeris accuracy and the correlation between the receiver clock offset and the float-valued carrier phase ambiguities in the real-time ODTS process.

Keywords Orbit determination · Time synchronization · LEO-PNT · Hardware-in-the-loop · CSAC

Introduction

Recent years have seen a rapid increase in research and development of positioning, navigation and timing (PNT) services from low Earth orbit (LEO). Various mega-constellations in LEO have been developed by space industry, with some of them already being deployed and operational. Space agencies are also working on enhancing the conventional GNSS constellations by additional LEO layers (Giordano et al. 2018; Priellec et al. 2025). These developments have mainly been driven by the continuous decrease in costs for launches to LEO, as well as the New Space approach of using cost-efficient and widely available commercial off-the-shelf (COTS) components instead of expensive space-grade hardware.

While different concepts and architectures have been proposed (Kozhaya et al. 2025; Eissfeller et al. 2024; Iannucci and Humphreys 2022; Psiaki 2021), proper knowledge of satellite orbits and clock offsets is a crucial aspect of any ranging-based LEO-PNT system. For the established GNSS constellations, the respective ground segments monitor the satellite orbits and realize a GNSS-specific system time scale. The GNSS satellite orbits and clock offsets determined and predicted on ground are uploaded to the GNSS satellites for transmission via the broadcast navigation messages. Based on these, users are then able to calculate the position and clock offset of the GNSS satellite at the transmission time of the ranging signal. The associated

✉ F. Kunzi
florian.kunzi@dlr.de

[1] Deutsches Zentrum für Luft- und Raumfahrt, German Space Operations Center, D-82234 Weßling, Germany

Published online: 16 October 2026

signal-in-space range error (SISRE) currently reaches 11 cm for Galileo and 26 cm for GPS, respectively (Montenbruck and Steigenberger 2025). For Galileo, recent studies have, furthermore, shown that the broadcast realization of the Galileo system time is consistent with the actual ground-based system time scale at the level of 0.5 ns RMS including mean offsets of less than about 0.2 ns (Montenbruck et al. 2025; Oliveira Salgueiro et al. 2026). For LEO-PNT systems, ground-based orbit determination and ephemeris generation can significantly increase the overall system complexity and costs due to the large number of satellites required for a global LEO-PNT constellation. Therefore, GNSS-based onboard orbit and time synchronization (ODTS) has become an important alternative for continuous and autonomous generation of satellite ephemerides.

Even though practical applications of GNSS-based onboard ODTS are still fairly limited, various studies processing actual flight data in play-back mode have previously demonstrated the feasibility of determining the orbits of LEO satellites in real-time with decimeter-level 3D RMS accuracy based on GPS and, preferably, Galileo observations and navigation data (Montenbruck et al. 2022; Hauschild et al. 2022; Kunzi et al. 2026b). Complementary to these, the performance of GNSS-based onboard time synchronization has been addressed in Kunzi and Montenbruck (2022), Montenbruck et al. (2025), and, most recently, Oliveira Salgueiro et al. (2026). The results obtained in these studies show that the achievable performance of GNSS-based onboard time-synchronization slightly falls behind the corresponding orbit determination performance. Processing both Galileo and GPS observations and broadcast navigation messages in a playback real-time navigation filter, representative accuracies of 0.70 ns (or, equivalently, 0.2 m) for the onboard time scale relative to Galileo system time have been obtained in those studies.

The use of GNSS observations from actual space missions in a play-back navigation filter provides important insights into the achievable onboard ODTS performance. However, it does not enable the characterization of a GNSS-disciplined oscillator controlled by the onboard ODTS process, which is of key interest as a low-cost alternative to high-grade atomic frequency standards in a LEO-PNT system. To cope with this limitation, this study presents a hardware-in-the-loop test enabling a fully integrated validation of GNSS-based real-time orbit determination, time synchronization, and oscillator disciplining. For this test, we make use of the ATOMIC (Autonomous Timing and Orbit determination for MIcrosatellite Constellations) payload developed by DLR as a prototype ODTS system for small satellites in LEO (Kunzi et al. 2023).

ATOMIC comprises a GNSS receiver, a micro-processor hosting the real-time ODTS filter, and a chip-scale atomic clock (CSAC), which is steered to the Galileo system time scale based on the outputs of the embedded navigation filter. Similar to the GNSS-disciplined CSAC presented in (Kunzi and Montenbruck 2023), the ATOMIC navigation filter makes use of precise carrier phase observations to improve the overall frequency stability but extends its application from terrestrial to orbital vehicles and provides a precise estimate of the host satellite's orbit and on-board time. Target applications include the use as an autonomous orbit determination system as well as a time and frequency source for transmitting GNSS-synchronized navigation signals for LEO-based GNSS augmentation in a layered system architecture. Aside from a small size, mass, and power consumption facilitating use on micro- and nanosatellites, ATOMIC offers a maximum degree of autonomy and thus helps to decrease the complexity of payload operations and ground segment.

The hardware-in-the-loop testbed developed for this study builds on a GNSS signal simulator and enables a thorough and highly realistic testing of GNSS-based onboard ODTS systems for LEO satellites including the combined assessment of orbit determination and time synchronization performance. On the example of the ATOMIC payload we de-monstrate that the performance previously found in offline data analyses can also be achieved in practice with representative flight hardware. Complementary to the real-time navigation solution, the GNSS-synchronized 10 MHz reference frequency output is monitored in real-time using a phase noise analyzer.

Following this introduction, the design and development of the ATOMIC payload are presented, including a general description of the navigation filter implementation and the clock steering process. Thereafter, the hardware-in-the-loop simulation environment as well as the evaluation methods are described. Subsequently, the results of both the orbit determination and the time synchronization are presented and discussed. Finally, a summary of the study results and related conclusions are given.

Real-time ODTS system

Within this study, the ATOMIC payload (Kunzi and Montenbruck 2023) is utilized as a representative implementation of GNSS-based ODTS system to assess the achievable orbit determination, time synchronization and frequency stability in a hardware-in-the-loop simulation. As illustrated in Fig. 1, the system is made up of a Septentrio AsteRx-m3 Pro+ GNSS receiver, an STM32H7 on-board computer (OBC), and a MicroSemi SA.45s chip-scale atomic clock (CSAC). Despite having a limited short-term stability, a CSAC has been selected for ATOMIC in view of its

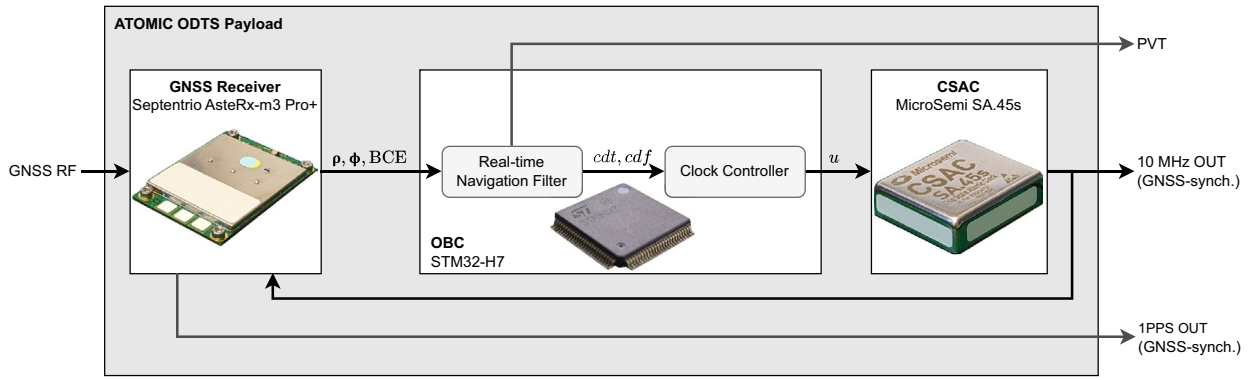


Fig. 1 Schematic of the ATOMIC payload and its time synchronization control loop. The GNSS receiver uses the CSAC as external frequency reference and provides measurements and broadcast ephemerides (BCE) to the real-time navigation filter, which computes a navigation solution including clock offset *cdt* and drift *cdf*. These parameters are used as input to the clock controller module, which computes a frequency steering command for the CSAC to synchronize its oscillator phase with Galileo system time

power consumption (0.12 W), which is one to two orders of magnitude smaller than that of more stable oven controlled crystal oscillators. Besides power and a telemetry/telecommand (TM/TC) interface, the payload only requires GNSS signals as an input for nominal operation. On the one hand, ATOMIC uses GNSS signals for a reduced dynamic orbit determination, which also serves as the basis for on-board ephemeris generation. On the other hand, the payload performs a time synchronization on hardware level leveraging the CSAC as local oscillator with a high short- and low long-term stability and the time information provided by GNSS broadcast ephemerides with a low short- and high long-term stability with respect to a global atomic time scale. More specifically, the payload performs a discrete steering of the CSAC's frequency towards a GNSS time scale, i.e., Galileo system time (GST) or GPS time (GPST). This process synchronizes the CSAC's relative phase and frequency with the respective GNSS time scale, ultimately improving the CSAC's long-term stability. The tight synchronization with GNSS time facilitates a seamless integration of a LEO-PNT satellite layer into existing GNSS constellations and a joint use of LEO-PNT signals and GNSS signals in a combined user receiver.

All computations required for the execution of the navigation filter and the clock steering in the ATOMIC system are performed on an embedded 32-bit STM32H7 microprocessor. The radiation tolerance of the processor and the proper function of its latch-up protection have been verified in dedicated total ionization dose and high-energy proton tests. At a 480-MHz clock rate and 1027 Dhrystone million instructions per second (DMIPS), the selected microprocessor provides adequate computing power for real-time navigation using fidelity models and algorithms.

Navigation filter

The ATOMIC real-time navigation software is based on state-of-the-art algorithms, which have been validated extensively in previous studies using flight data from actual space missions (Montenbruck and Ramos-Bosch 2008; Hauschild and Montenbruck 2021; Darugna et al. 2022; Oliveira Salgueiro et al. 2026). An extended Kalman filter is employed to process ionosphere-free combinations of dual-frequency GNSS code and carrier-phase measurements along with a reduced dynamic orbit model (Wu et al. 1991) and provides improved estimates of the state vector

$$\mathrm{x} = [\mathrm{r}; \mathrm{v}; cdt; cdf; \mathrm{ISB}; \mathrm{a}_{\mathrm{emp}}; C_D; C_R; \mathrm{A}_{\mathrm{amb}}] \quad (1)$$

at each measurement epoch. Here, r and v are the position and velocity of the satellite's center of mass (COM) expressed in the Geocentric Celestial Reference Frame (GCRF). The clock offset *cdt* and drift *cdf* describe the CSAC's phase and frequency offset with respect to Galileo system time (GST) in units of distance and distance rate, respectively. To account for the system time differences between GST and GPS time (GPST), an inter-system bias (ISB) is estimated as well. For the force model, empirical accelerations $\mathrm{a}_{\mathrm{emp}}$ as well as the atmospheric drag and solar radiation pressure (SRP) coefficients are estimated, here denoted as C_D and C_R, respectively. For each tracked GNSS satellite, the filter also estimates a float-valued carrier phase ambiguity as part of the vector $\mathrm{A}_{\mathrm{amb}}$. To improve the overall filter performance in the presence of broadcast ephemeris errors, we account for complementary white process noise in these states. The resulting "pseudo-ambiguities" lump the actual carrier phase ambiguities with signal-in-space range errors (SISRE) and offer a lean way of compensating those errors without introducing dedicated SISRE states in the

filter (Montenbruck and Ramos-Bosch 2008; Wang et al. 2015).

Within the time update step of the Kalman filter, the carrier phase ambiguities, clock drift, and ISB are propagated as constants with white process noise to the next measurement epoch, while a linear model incorporating the clock drift is used for the clock offset. Float ambiguity initialization for rising satellites is performed using code-minus-carrier and a large a priori variance. As further described in the next section, the CSAC is controlled based on frequency steering commands. Therefore, the control input u from the last measurement epoch is added to the propagated clock drift. The empirical accelerations are updated using an exponential decay model (Kunzi et al. 2026b). For the prediction of the satellite state vector $\mathrm{y} = (\mathrm{r}; \mathrm{v})$, the equation of motion

$$\dot{\mathrm{y}} = \begin{pmatrix} \mathrm{v} \\ \mathrm{a} \end{pmatrix} \tag{2}$$

is solved using a fifth-order Dormand-Prince (DP5; Dormand and Prince 1980 numerical integrator. A reduced dynamic orbit model is used to describe the satellite's acceleration a considering the Earth's gravitational potential, solid Earth tides, luni-solar gravity, atmospheric drag, and SRP, as well as the empirical accelerations $\mathrm{a}_{\mathrm{emp}}$. Further details of the individual contributions are given in Table 1. The state transition and sensitivity matrices providing the partials of the satellite state vector with respect to the initial state and the various force model parameters are obtained by numerical integration of a tailored set of variational equations (Montenbruck and Gill 2000; Montenbruck and Ramos-Bosch 2008).

Table 1 State estimation and force modeling of real-time navigation filter implemented on ATOMIC for use within this study

Item	Real-time ODTS payload
Estimation	Extended Kalman filter
GNSS measurement rate	30 s
Carrier-phase ambiguities	Float
Earth gravity model	GOCO03S, 70x70 (Mayer-Gürr et al. 2012)
Solid Earth tides	k_2 tides (Rizos and Stolz 1985)
Ocean tides	neglected
Third-body gravity	Low-precision coordinates for Sun and Moon (Montenbruck and Gill 2000)
Atmospheric drag	cannon-ball model; Harris-Priester atmospheric density model (Harris and Priester 1962)
Solar radiation pressure	cannon-ball model; constant radiation
Earth radiation pressure	neglected
Observations	Code and phase; GPS (L1 C/A, L2C), Galileo (E1C, E5a)
Receiver antenna	nominal phase center location
Attitude	nominal Earth-pointing
Process noise emp. accel	$\sigma_{\mathrm{emp}} = (1.5, 8.0, 15.0)$ nm/s^2 for RAC axes, $\tau_{\mathrm{emp}} = 600$ s
Process noise ambiguities	Galileo $q_A = (7\,mm)^2/30\,s$, GPS $q_A = (20\,mm)^2/30\,s$

For the measurement update, the filter processes ionosphere-free dual-frequency combinations of code and carrier phase observations. The measurement equations for pseudorange and carrier phase of the n-th GNSS satellite of constellation g are expressed as

$$\rho^n = ||\mathrm{r}_{\mathrm{APC}} - \mathrm{r}^n|| + (cdt - cdt^n) + \mathrm{ISB}_g + B^n \tag{3}$$

and

$$\phi^n = ||\mathrm{r}_{\mathrm{APC}} - \mathrm{r}^n|| + (cdt - cdt^n) + \mathrm{ISB}_g + A^n_{\mathrm{amb}}\,, \tag{4}$$

respectively. Here, r^n and cdt^n are the light-time corrected antenna phase center position and clock offset of the GNSS satellite at the measurement epoch as obtained from the broadcast ephemeris. The position of the LEO satellite antenna phase center $\mathrm{r}_{\mathrm{APC}}$ is obtained from the estimated center-of-mass position r taking into account the satellite-specific attitude and the antenna offset in the spacecraft body system. For consistency with the GNSS satellite positions obtained from the broadcast ephemerides, the LEO satellite position in the observation model is likewise expressed in the Earth-fixed International Terrestrial Reference Frame (ITRF). The carrier phase model considers the respective float ambiguity A^n_{amb} estimated by the navigation filter.

By convention, the receiver clock offset of the ATOMIC navigation filter is referred to Galileo System Time and the ionosphere-free E1/E5a signal combination. As such, the observation model takes into account a complementary inter-system bias $\mathrm{ISB}_{\mathrm{GPS-GAL}}$ for all GPS satellites. In addition, a signal- and satellite specific differential code bias B^n is taken into account in the pseudorange observation model. For GPS, this bias is obtained from the timing group delay (TGD) and inter-signal correction (ISC) parameters of the CNAV navigation message (Tetewsky et al. 2009). More specifically, the code bias combination

$$B^n = +c \cdot \mathrm{TGD}^n - \frac{c}{\gamma - 1}\left(\gamma \cdot \mathrm{ISC}^n_{\mathrm{L1CA}} - \mathrm{ISC}^n_{\mathrm{L2C}}\right) \tag{5}$$

(Montenbruck and Hauschild 2013; Montenbruck et al. 2018) needs to be considered for the civil L1 C/A and L2C GPS signals tracked by the ATOMIC GNSS receiver. Here, c denotes the speed of light and $\gamma = f^2_{\mathrm{L1}}/f^2_{\mathrm{L2}}$ is the squared ratio of the L1 and L2 signal frequencies. For Galileo, on the other hand, no code biases need to be applied when using the E1/E5a signals together with Galileo satellite clock offsets from the F/NAV navigation message and the ISB vanishes by default.

Further data beyond the broadcast ephemerides required by the filter are obtained from the GPS CNAV navigation message. This includes Earth orientation parameters (EOPs) as well as UTC information. Following the measurement update, the estimated GCRF-based position and velocity are transformed to the ITRF and transmitted as part of the ATOMIC telemetry. This transformation makes the resulting navigation solution largely insensitive to errors in the employed EOPs and facilitates a direct comparison with the simulation truth trajectory of or precise orbit determination (POD) solutions obtained in post-processing from the collected GNSS observations.

In accord with the orbital dynamics, filter update intervals of 10–60 s are fully sufficient to obtain smooth and accurate estimates of the LEO trajectory from onboard GNSS measurements. As such, the update interval for the ATOMIC system is driven by the dynamics of the clock state and the need to tightly control the clock offset with respect to Galileo system time. Given the short term stability of the employed CSAC clock, update intervals of 10–30 s provide a reasonable compromise between computational effort and the achievable control accuracy for the oscillator disciplining. For all test described in this study, the ATOMIC navigation filter was operated at a 30 s update interval.

Oscillator disciplining

Within the ATOMIC ODTS system, the CSAC serves as an external frequency reference for the GNSS receiver (c.f. Fig. 1). The CSAC's short-term stability is in the order of $10^{-10}/\sqrt{\tau/\mathrm{s}}$ over time intervals τ of less than 1000 s (Lutwak et al. 2007; Lutwak 2011). As shown in Kunzi and Montenbruck (2023), this is roughly comparable to the short term stability of GNSS based clock offset estimates obtained in a carrier-phase processing with GNSS broadcast ephemerides. However, over longer time intervals, the oscillator's clock phase tends to drift with respect to stable atomic time scales such as Galileo system time (GST) and GPS time (GPST). To compensate the long-term drift and simultaneously benefit from the high short-term stability, the CSAC can be disciplined with respect to GNSS time (Lombardi 2008, 2016). Kunzi and Montenbruck (2023) have earlier shown that a sub-nanosecond time synchronization precision with respect to GNSS time can be achieved in a static terrestrial scenario over multiple days when using carrier-phase precise point positioning (PPP) with broadcast ephemerides. The ODTS system for LEO satellites assessed in the present study inherits the clock controller concept developed in that work. It is based on a time-discrete linear-quadratic regulator (LQR; Levine 2019) and leverages the CSAC's phase and frequency deviation estimated by the navigation filter as clock offset and drift. As the CSAC accepts relative frequency steering commands, the clock controller needs to provide delta frequency values which ultimately drive the CSAC's relative phase towards the reference time scale. Therefore, the control law for the steering process becomes

$$u_i = -\mathrm{G} \cdot \begin{pmatrix} cdt_i \\ cdf_i \end{pmatrix} \tag{6}$$

and yields a discrete steering value u_i for epoch i, which is commanded to the CSAC as depicted in Fig. 1. The control gain G is a two-element column vector, with its derivation further described in Kunzi and Montenbruck (2023). As the clock control process relies on the state estimation of the navigation filter to obtain the instantaneous clock offset and drift parameters, the maximum control rate is ultimately tied to the navigation filter's measurement update rate. Note that the controller only performs a relative phase alignment with respect to the reference oscillator, as otherwise a complex hardware calibration would need to performed which is out of scope for this study.

Simulation and test concept

While previous studies of GNSS-based onboard ODTS have mostly focused on play-back processing of GNSS data collected in various LEO missions, these simulations cannot cover the aspects of data real-time processing and, in particular, a real-time clock steering. To overcome these limitations, a hardware-in-the-loop (HIL) test bed has been established in the present work, which enables validation of actual ODTS hardware and is applied here to the ATOMIC payload.

Hardware-in-the-loop test bed

At its core, the HIL test bed illustrated in Fig. 2 comprises a GNSS signal simulator generating GNSS signals representative of those received by a LEO satellite. These signals are fed to the antenna port of the ODTS unit, which tracks those signals with the built-in GNSS receiver and uses the resulting measurements for real-time orbit determination and time synchronization. For a direct monitoring of the GNSS-disciplined oscillator within the ODTS unit, the test bed includes a phase noise analyzer (PNA), which compares the ODTS frequency output against the oscillator of the signal simulator that defines the simulation truth time. In addition, the ODTS performance can be evaluated with the payload's real-time navigation solution and the raw GNSS observables collected as part of the ODTS telemetry.

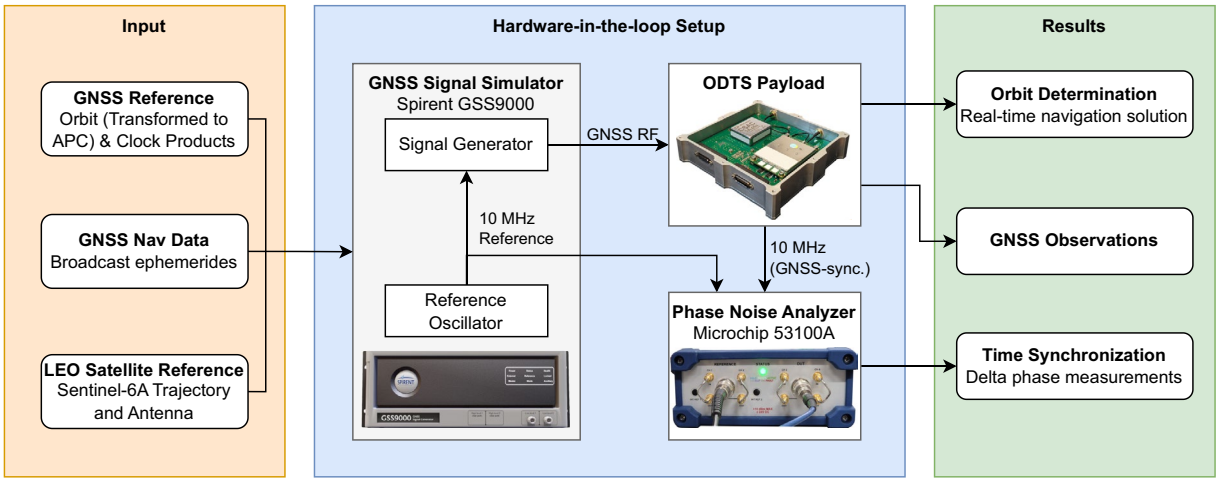


Fig. 2 Hardware-in-the-loop setup including GNSS signal simulator, ATOMIC payload and a frequency counter. The payload's disciplined 10 MHz output is compared against the signal simulator's frequency reference to assess the time synchronization performance

For completeness, we note that no effort is presently made to assess the absolute timing accuracy of the ODTS payload, which would require dedicated calibrations of signal-specific code biases and the 1-PPS signal of the employed GNSS receiver as well as the simulation hardware. As such, all timing results presented in this study are subject to possible biases that would aggregate with signal generation biases in an actual LEO-PNT system and would have to be determined in an end-to-end bias calibration.

Despite the conceptual simplicity of the HIL test bed, its practical use and the values of the collected performance data depends crucially on the capability of the employed GNSS signal simulator to provide a highly realistic signal in space that is fully representative of an actual LEO mission and the present GNSS systems. In particular, this requires the simulation of a user trajectory consistent with the actual LEO orbit dynamics, GNSS orbit and clock offsets representative of the true constellations as well as the transmission of broadcast navigation message reflecting the current SISRE performance. A dedicated effort has therefore been made to drive the employed signal simulator with real trajectory and constellation data wherever possible. Remaining limitations relate to the lacking simulation of transmit and receive antenna phase patterns and phase wind-up as well as restrictions in the application of signal-specific code biases. However, neither of these is considered to affect the overall realism of the simulation and the credibility of the obtained ODTS performance results.

Test scenario

Table 2 shows the general properties and inputs to the GNSS simulator adopted in the present test. The simulation covers GPS and Galileo signals and is performed over 24 h for 2 August 2025, using the LEO spacecraft Sentinel-6A (S6A) at an altitude of 1336 km as a test case. This altitude is considered representative of candidate LEO-PNT constellations in the upper LEO regime (Eissfeller et al. 2024), which aim to minimize atmospheric drag and to maximize the visibility duration for ground-based users. The reference trajectory

Table 2 Simulation environment and configuration

Item	Description
Simulation time	24 h on 2 August / day of year (DOY) 214, 2025
Simulation hardware	Spirent GSS9000
GNSS simulation	
Constellations	Galileo + GPS
Signals	Galileo E1 O/S, E5a GPS L1 C/A, L2C
Reference orbits	CODOPSFIN (Dach et al. 2024), transformed from COM to APC and interpolated to 30 s stepsize
Reference clocks	CODOPSFIN with 30 s stepsize
Code biases	no group delays in R/F signal, random group delays (0.3 ns 1-σ) in $ISC_{C/A}$ and ISC_{L2C} of CNAV navigation message
Antenna offsets	I20_2388.ATX
Antenna phase patterns	neglected
Navigation data	Galileo F/NAV, GPS LNAV/CNAV (Montenbruck and Steigenberger 2022)
Ionospheric path delays	NeQuick-G model
LEO spacecraft simulation	
Spacecraft	Sentinel-6A, 1,336 km altitude (Donlon et al. 2021)
Reference orbit (COM)	Sentinel-6A POD (Fernández et al. 2024; EU 2026)
Attitude	Quaternions (EU 2026)
Antenna offset from COM	$(+0.9419, +0.0071, -1.1173)$ m
Antenna phase patterns	neglected
Antenna gain patterns	Extended patch excited cup antenna (Öhgren et al. 2011)

of S6A is based on a post-processed POD provided by the Copernicus POD (CPOD) service (Fernández et al. 2024) and reflects the real-world orbital dynamics including the full set of gravitational and non-gravitational forces acting on a representative spacecraft at that altitude. Along with onboard attitude quaternions (EU 2026) describing the inertial orientation of the spacecraft body frame as well as the antenna phase center offset from the center of mass, the position of the receiving GNSS antenna is modeled in the simulator in close accord with the true Sentinel-6A mission. For a representative simulation of the received signal power and carrier-to-noise density, gain patterns of the Beyond Gravity (formerly RUAG) extended patch excited cup antenna (Öhgren et al. 2011) are adopted.

The performance of any GNSS-based real-time navigation system is largely dependent on the signal-in-space range error associated with the transmitted broadcast navigation messages. As such, substantial care is taken in the simulation to achieve a realistic SISRE that is fully representative of the GNSS system performance on the day of interest (Montenbruck et al. 2018; Montenbruck and Steigenberger 2025). This is achieved by combining high-fidelity GNSS orbit and clock offset values for the signal simulation with the actual broadcast navigation messages transmitted on the day of interest.

The true constellations of both Galileo and GPS are simulated based on final orbit and clock products from the Center for Orbit Determination in Europe (CODE; Dach et al. 2024). For use within the signal simulator, the COM-referenced precise orbit products are transformed to the antenna phase center (APC) using the conventional antenna models of the International GNSS Service (IGS; Johnston et al. 2017) satellite specific models of the nominal and rate limited yaw-steering (Montenbruck et al. 2015).

The GNSS satellite clock offsets introduced in the simulation environment are obtained from the CODE clock products and thus consistent with the APC-referenced CODE orbits. It must be noted, though, that the system time scale of the CODE clock products represents a proprietary, product-specific time scale which is conceptually different from the true GPS and Galileo system time scales (GPST, GST) that serve as reference for the broadcast ephemerides transmitted in the simulation. The corresponding differences are typically at the few-nanosecond-level (Dach et al. 2015) and can essentially be considered as constant over the one-day simulation period. Since the real-time navigation system will align the onboard time scale to the time system of the primary GNSS (here, Galileo) as realized by the respective broadcast navigation data, a systematic bias between the estimated and the simulated time scale can ultimately be expected that reflects the CODE-minus-Galileo system time difference. On the other hand, the assessment of the overall precision of the time synchronization and the stability of the GNSS disciplined oscillator (as obtained, for example, from the phase noise analyzer measurements) remains unaffected by this simulation-related system time bias.

The precise orbit and clock products used to define the transmitted GNSS signal within the simulation are complemented by broadcast ephemerides closely replicating the content and scheduling of the real broadcast navigation messages transmitted by the Galileo and GPS satellites on the day of interest. The respective orbit and clock parameters as well as auxiliary parameters such as leap seconds, system time offsets, ionosphere model parameters, and EOPs are obtained from the BRD4 product (Montenbruck and Steigenberger 2022) of the IGS, which provides daily records of the various types of navigation messages transmitted by the present GNSS satellites as well as their time of first transmission. Depending on the constellation, the to-be-transmitted navigation messages of the simulator are either specified by interval-wise parameter sets (GPS LNAV and CNAV) or the bit-patterns of the individual messages (Galileo I/NAV and F/NAV). By combining precise GNSS orbit/clock products for the simulator configuration with actual navigation data, a close-to-real SISRE of the simulated GNSS signals is ensured, which enables a highly realistic testing of real-time ODTS for LEO satellites.

As a minor limitation to the concept of highest realism, signal-specific group delays in the simulated signals have been set to zero due to limited flexibility for application of independent code and phase delays in the employed signal simulator. As a workaround, the GPS navigation messages for the simulated signal have been populated with randomized values of the TGD and ISC parameters. These mimic a roughly 1 ns (1-σ) uncertainty of the $B^{\mathrm{L1CA,L2C}}$ bias (cf. Equation (5)) applied by the navigation system relative to the truth values and contribute to the signal-in-space-range error of the simulated signal. For Galileo, broadcast group delay (BGD) uncertainties do not affect the positioning when working with E1/E5a signals and F/NAV navigation message. As such, no BGD errors are applied in our simulation. The overall global-average SISRE implemented in the present tests amounts to 0.45 m for GPS L1CA/L2C and 0.12 m for Galileo F/NAV use in close accord with the true SISRE values on the day of interest of 0.43 m and 0.10 m, respectively.

Performance assessment concept

The hardware-in-the-loop test bed enables a comprehensive evaluation of navigation solution and the time synchronization achieved with a flight-representative real-time ODTS system. In principle, the ODTS performance analysis is based on comparison with the simulation truth, but different

approaches are required for the analysis of the navigation and timing characteristics.

For the assessment of the real-time orbit determination performance, the position solution of the navigation filter provided via the telemetry interface of the ATOMIC unit is utilized. The ITRF positions obtained after each measurement epoch refer to the satellite's COM, which enables a direct comparison against the reference trajectory used in the signal simulator without further transformations.

It may be noted, though, that the one-to-one comparison with the reference trajectory of the test scenario is contaminated by the presence of subtle timing biases which give rise to apparent along-track errors in the measured positions. Previous analyses of signal simulator tests for spaceborne GNSS receivers have revealed total errors of about 1–3 µs (Montenbruck et al. 2006), which mimic along track errors of about 1–2 cm and may include joint contributions of the receiver (Calliess et al. 2024) and the signal simulator. In the present test setup, a total error of − 2.3 µs has been observed, which can largely be attributed to the employed simulator, while receiver-related contributions are expected to be less than 0.5 µs based on comparison with a variety of other current space receivers.

To evidence these errors and to compensate them in the performance analysis, we generated a reference trajectory in post-processing based on the GNSS observations of the ODTS system collected in the HIL test. For this purpose, the pseudorange and carrier phase observations were processed in a batch POD system (Montenbruck et al. 2021) using high-fidelity orbit and observation models with ambiguity fixing (Table 3) along with precise GNSS orbit, clock, and bias products as used in the scenario configuration. The comparison of this solution against the reference trajectory (Fig. 3) clearly shows a −16.8 mm along-track bias which notably exceeds the overall POD uncertainty and is related to the aforementioned timing bias. This bias is mostly related to the fact that the simulated signal dynamics exhibits a roughly 2 µs latency with respect to the transmit time information modulated on the signals themselves. By comparing the real-time navigation solution against the POD solution obtained from the recorded GNSS observations rather than the LEO trajectory used in the simulator configuration, an unbiased performance estimate relative to the simulation truth can be obtained. As a by-product, the POD solution obtained from the recorded GNSS observations of the HIL test also provides a complementary reference for the clock analysis as will be further described below.

Within the simulation environment illustrated in Fig. 2, all GNSS signals are coherently generated from the internal, oven controlled crystal oscillator (OCXO) of the signal simulator. The associated system time scale is realized through modulation of the transmitted signals with satellite-specific time stamps and ranging code offsets as defined by the satellite clock offset values adopted in the configuration of the simulation scenario (Table 2). A GNSS receiver connected to the simulator will ideally determine the receiver clock offset with respect to this simulation time scale and a GNSS disciplined oscillator will ideally output a clock phase and frequency aligned to the OCXO signal and the simulation system time scale. However, as no calibration is performed, an arbitrary phase offset will remain between the steered oscillator and the simulation reference. For completeness, we also note that any possible imperfections of the simulator's OCXO only affect the relation between the simulation time scale and the real-world time scale, but do not impact the analysis of the GNSS-based time synchronization within the test bed.

Table 3 State estimation and force modeling of batch least-squares filter employed for obtaining a post-processed reference clock solution

Item	Post-processing
Estimation	Batch least squares
GNSS measurement rate	30 s
Carrier-phase ambiguities	Fixed to integer values
Earth gravity model	GOCO06S, 70 × 70 (Kvas et al. 2020)
Solid Earth tides	IERS2003
Ocean tides	FES2014b ocean tide model (Lyard et al. 2021)
Third-body gravity	Point mass model with analytical series for Sun and Moon coordinates
Atmospheric drag	S/C macro model; NRLMSISE-00 atmospheric density model (Picone et al. 2002)
Solar radiation pressure	S/C macro model
Earth radiation pressure	S/C macro model; CERES Earth radiation model (Loeb et al. 2018)
Relativity	Post-Newtonian correction
Earth orientation parameters	IGS final products

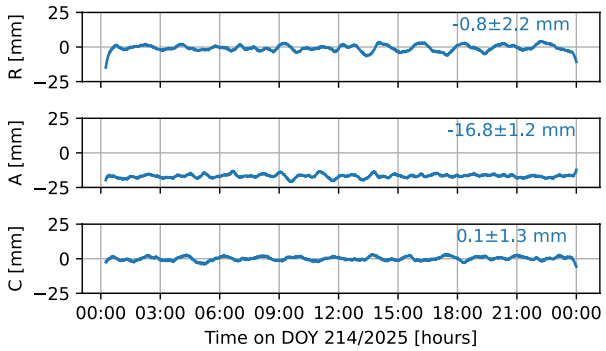


Fig. 3 Differences between the post-processed precise orbit determination using GNSS measurements recorded in the HIL test and the reference trajectory used in the simulator configuration. Labels in the subplots denote the mean ± standard deviation or errors in radial, along- and cross-track direction

The chosen architecture of the HIL test bed supports two independent but complementary approaches for the analysis of the achievable onboard time synchronization. In a first step, the steered 10 MHz output of the ODTS system is evaluated using a PNA as shown in Fig. 2. It measures the relative phase offset from the reference signal of the signal simulator's OCXO and enables a direct verification of the GNSS-synchronized frequency output on hardware level. In a LEO-PNT system, the frequency output of the ODTS subsystem would serve as reference for the LEO-PNT signal generation. The HIL testing thus offers a unique opportunity for pre-flight validation of the GNSS-based oscillator disciplining and an assessment of the associated timing errors for LEO-PNT users.

As a second method for evaluating the time synchronization error of the ODTS system, the post-processed POD solution described above is again employed. Within this POD, epoch-wise receiver clock offsets are determined from GNSS observations collected during the test. The POD makes use of the simulation-truth GNSS orbit and clock products and ultimately provides the difference between the receiver time scale (i.e., the clock phase of the steered oscillator) and the simulation time scale (i.e., the phase of the simulator's master oscillator). This approach matches the analysis concept used in previous studies for the assessment of time synchronization performance (Kunzi and Montenbruck 2022; Montenbruck et al. 2025). Other than the PNA measurements, this concept does not require direct access to the oscillator and can likewise be used for in-orbit testing based on GNSS flight data recorded during operation of an ODTS payload. As will be shown below, the GNSS data analysis delivers closely matching results in terms of relative phase error compared to the PNA evaluation, which provides further justification for using for time synchronization performance validation in actual LEO-PNT missions.

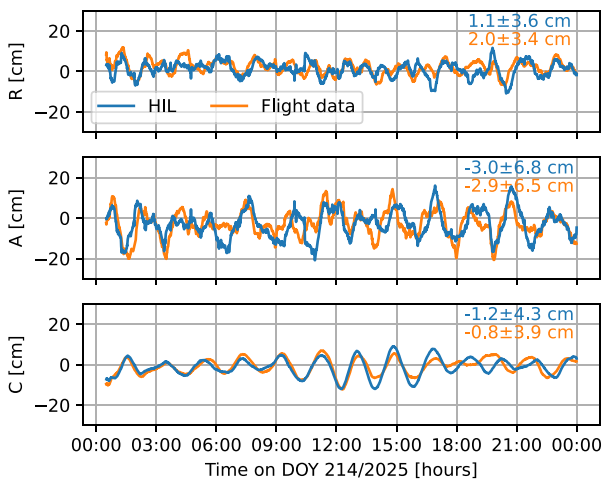


Fig. 4 Errors of the real-time navigation filter with respect to the reference trajectory of Sentinel-6A on DOY 214/2025. Labels in the subplots denote the mean ± standard deviation or errors in the RAC frame. The 3D RMS position error over the 24-h arc amounts to 9.5 cm and 9.0 cm for the solutions obtained with simulated and real flight data, respectively

Results and discussion

Orbit determination

The orbit determination results of the real-time navigation filter are obtained directly from the ODTS system's telemetry and compared against the POD-based simulation-truth trajectory as described in the previous section. The respective real-time orbit errors in RAC frame are presented in Fig. 4 in blue, with an overall 3D root mean square error of 9.5 cm. The results exhibit a performance level comparable to previous studies on real-time orbit determination of Sentinel-6A using actual GPS and Galileo observations (Darugna et al. 2022; Montenbruck et al. 2022; Kunzi et al. 2026b) and are dominated by errors in the along-track and cross-track axes with characteristic once-per-revolution oscillations (Colombo 1989).

For an additional assessment of the simulation's realism, observables obtained from real flight data of Sentinel-6A on the same day were utilized in a play-back real-time navigation filter similar to the one implemented in the ODTS system. The results depicted in orange in Fig. 4 show a good agreement with the simulated data as well as a similar 3D RMS error of 9.0 cm over the 24-h evaluation period. The discrepancies between the real-time navigation solutions of simulated and real flight data can largely be attributed to differences in the measurement quality of the employed GNSS receivers, including the presence of small time varying pseudorange biases in the S6A flight data. Nevertheless, the good overall match of confirms a high level of realism of the HIL simulation with respect to the orbital dynamics and GNSS signal conditions in representative LEO missions.

Time synchronization

A direct assessment of the time synchronization is performed using the relative phase deviations between the payload's steered 10 MHz output and the GNSS signal simulator's reference frequency as measured by the PNA in real-time. For an independent verification, clock offsets obtained in post-processing from a reference POD are evaluated. The results of both methods are shown in the upper panel of Fig. 5. As only the relative phase offset is assessed, both time series were adjusted to zero mean, and displayed with offsets of ±3 ns for improved readability. It can be seen that both results follow the same trend with long-term changes of about ±1 ns and noise-like short-term of a similar magnitude.

Taking the difference between the two time series results in an error with a standard deviation of around 37 ps, or, equivalently, 11 mm as depicted in the lower panel of Fig. 5. This includes a short-term noise of about 10 ps (3 mm) similar to the noise level of the carrier-phase-based POD clock offset estimates. Superimposed to these systematic differences of up to ±100 ps (33 mm) may be observed over the 24 h evaluation period, which most likely reflect the stability of temperature dependent biases in the current measurement setup.

Overall, the two approaches exhibit a good consistency in line with the needs of validating the performance of GNSS-disciplined oscillators for LEO-PNT systems. Most importantly, the results demonstrate that the POD-based time synchronization assessment (Montenbruck et al. 2025) offers a trustworthy alternative to hardware-based measurements that are naturally limited to ground testing but can't be applied to flight data analyses.

The frequency stability of the ATOMIC clock signal as measured in the HIL test is depicted in terms of the overlapping Allan deviation (OADEV; Allan 1966) and the time deviation (TDEV) in Figs. 6 and 7, respectively. For further comparison, the OADEV plot also provides the stability of the free-running CSAC, which exhibits a roughly three times better performance than specified by the manufacturer (Microchip Technology Inc 2019). Without steering, the distinctive $\tau^{-1/2}$ trend indicates that white frequency modulation (FM) noise dominates at time intervals lower than 10^3 s, until the flicker noise floor is reached and the long-term stability decreases (Riley and Howe 2008). For the steered CSAC, the OADEV shows the same stability for time intervals lower than 10 s. Here, the native stability of the CSAC is observed, as the clock runs freely between two measurement epochs. Around $\tau = 30$ s, a slight degradation in stability of the steered clock can be observed. This phenomenon is caused by the discrete clock steering process, which occurs at every measurement epoch, i.e., once every 30 s. For longer time intervals beyond 100 s, the CSAC's frequency is steered towards the Galileo broadcast time scale as reconstructed from the satellite clock offsets of the broadcast ephemerides, and the noise transitions to white or flicker phase modulation (PM) noise.

The overall time synchronization performance is on the one hand limited by the quality of the respective broadcast ephemerides, which provide an approximation of the actual GNSS system time scale. On the other hand, the performance of a real-time navigation filter estimating float ambiguities as used in the ATOMIC system suffers from a correlation between the clock offset and carrier phase ambiguity estimation (Montenbruck et al. 2025). Finally, the clock steering process itself is limited by uncertainties in the hardware frequency steering. This ultimately leads to a time synchronization precision of the CSAC's relative

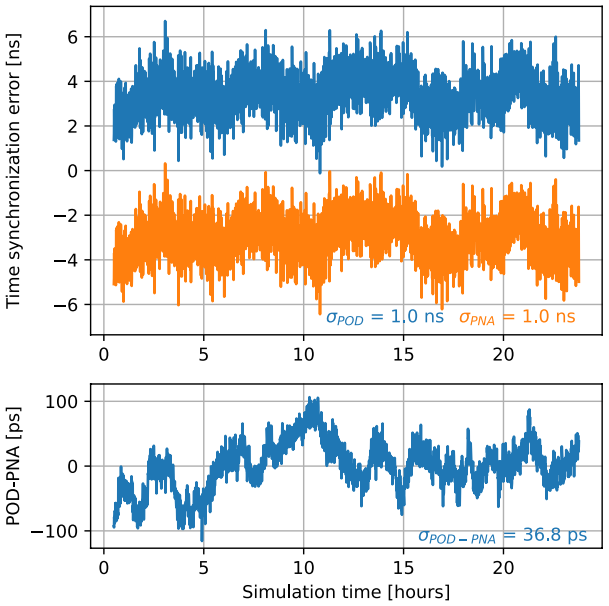


Fig. 5 Results of the clock steering, omitting the first 30 min of navigation filter convergence phase. Upper plot: Relative phase deviation of CSAC obtained with the PNA as well as with the post-processed POD. Both solutions are adjusted to zero mean and depicted with ±3 ns offsets. Lower plot: Difference between POD and PNA results after zero-mean alignment

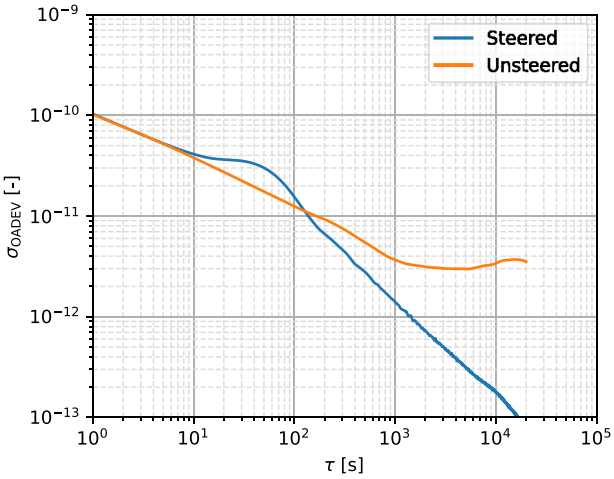


Fig. 6 Stability of the phase error measured by the PNA in terms of overlapping Allan deviation. Curves for both GNSS-synchronized and free-running CSAC are given to show the impact of the clock steering

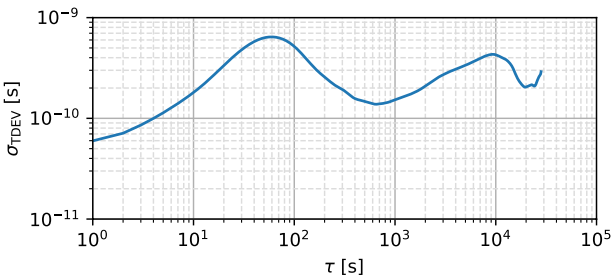


Fig. 7 Time deviation of the phase error measured by the PNA

phase of about 1.0 ns with respect to the system time scale. This value is comparable to previous results in a terrestrial receiver setup (Kunzi and Montenbruck 2023), which again validates the realistic conditions provided by the hardware-in-the-loop environment.

Summary and conclusions

This study presents a hardware-in-the-loop environment, enabling pre-flight testing of an ODTS payload for LEO satellites under highly realistic GNSS signal conditions. The simulation environment utilizes a GNSS signal simulator generating GPS and Galileo signals for a LEO spacecraft trajectory, which replicates the orbital dynamics of an actual space mission. By way of example, the orbit of Sentinel-6A on 2 August 2025 as derived from a precise orbit determination is employed for this purpose to facilitate the comparison of laboratory tests with actual flight data. A fully representative signal-in-space range-error budget in the HIL test bed is ensured by using real GNSS orbits and clock offsets as well as broadcast navigation messages for the day of interest in the configuration of the simulation scenario. With this setup, a full ODTS chain including oscillator disciplining can be verified with a high level of realism in real-time.

To demonstrate the capabilities of the test environment, the ATOMIC system is utilized as a representative GNSS-based ODTS system. The real-time orbit determination performance is assessed by comparing the payload's navigation solution with the simulation-truth reference trajectory. The results yield a 3D orbit RMS of approximately 9.5 cm and an error distribution in the radial, along-track and cross-track directions well comparable to results obtained with real Sentinel-6A flight data. For the assessment of the time synchronization performance, two independent methods are utilized. On the one hand, the GNSS-synchronized 10 MHz output of the ATOMIC time synchronization subsystem is directly compared with the reference frequency of the signal simulator using a phase noise analyzer. On the other hand, the ATOMIC GNSS observables recorded during the test are post-processed in a batch least-squares POD to obtain the onboard clock error with respect to the reference time scale. Both methods yield relative phase errors of the payload's CSAC with a precision of around 1.0 ns over the 24 h evaluation period, and coincide within 37 ps (1-σ).

The results of both the real-time orbit determination and the real-time time synchronization achieved by the ATOMIC system in the present tests are well consistent with previous performance studies using actual LEO GNSS data (e.g., Darugna et al. (2022), Montenbruck et al. (2022), and Kunzi et al. (2026b)). This shows that the presented hardware-in-the-loop test environment provides highly realistic conditions for the testing and pre-flight validation of an actual ODTS payload. On the other hand, the aforementioned studies are entirely based on playback processing of flight data. Therefore, they are limited to accuracy validations of the employed real-time navigation algorithms, but could not address the feasibility and run-time performance of real-time processing in an embedded computer system for space applications. The results of this study now verify that a GNSS-based real-time orbit determination at decimeter-level is indeed possible with a dedicated space hardware despite its limited processing power.

High-precision GNSS-based time synchronization at hardware level using a steered CSAC could only be demonstrated so far in a static terrestrial setup (Kunzi and Montenbruck 2023). This study now shows that oscillator disciplining and time synchronization can also be performed in real-time onboard of a LEO satellite with a precision at the one-nanosecond level. Furthermore, the study demonstrates a high level (37 ps std. dev.) of consistency between clock phase measurements obtained by a phase-noise analyzer and clock offsets derived from GNSS observations in a post-processed precise orbit determination. It thus confirms the validity of POD-based concepts for assessing the time-synchronization of onboard ODTS systems as studied in (Kunzi and Montenbruck 2022; Montenbruck et al. 2025; Oliveira Salgueiro et al. 2026) and proposed for validation of future LEO-PNT systems.

Future work will address the incorporation of corrections from the Galileo High Accuracy Service into the simulation environment. These corrections promise a further performance improvement for GNSS-based LEO ODTS systems (Kunzi et al. 2026a). The extension to Galileo E6 signals and the use of actual HAS data in the simulation will enable a fully realistic testing of HAS-enabled ODTS terminals for LEO satellites in support of the design and build up of future LEO-PNT systems.

Acknowledgements The authors would like to thank the Signal Analysis and Timing Systems Department of DLR's Galileo Competence Center for the provision of the phase noise analyzer, the Center of Orbit Determination in Europe (CODE) for the precise GNSS products, as well as the Copernicus POD (CPOD) service for the Sentinel-6A spacecraft data used in this study. GNSS navigation messages used in this study were kindly provided by the IGS. The support of all station providers, analysis centers and data centers is gratefully acknowledged.

Author contributions FK proposed the study concept, prepared the draft manuscript, conducted the data analysis, and generated all figures and illustrations. JH prepared and verified the simulation environment. OM reviewed the methodology and results and contributed to their discussion. All authors critically reviewed the final manuscript.

Funding Open Access funding enabled and organized by Projekt DEAL, an initiative of the Alliance of Science Organisations in Germany.

Data availability GNSS navigation data as used in this study are publicly available from the global data centers of the International GNSS Service (IGS), such as CDDIS (https://cddis.nasa.gov/archive/gnss/data). All data for Sentinel-6A used in this study are publicly available at the Copernicus Data Space Ecosystem (https://dataspace.copernicus.eu/)

Declarations

Conflict of interest The authors have no conflict of interest that are relevant to the content of this article.

Open Access This article is licensed under a Creative Commons Attribution 4.0 International License, which permits use, sharing, adaptation, distribution and reproduction in any medium or format, as long as you give appropriate credit to the original author(s) and the source, provide a link to the Creative Commons licence, and indicate if changes were made. The images or other third party material in this article are included in the article's Creative Commons licence, unless indicated otherwise in a credit line to the material. If material is not included in the article's Creative Commons licence and your intended use is not permitted by statutory regulation or exceeds the permitted use, you will need to obtain permission directly from the copyright holder. To view a copy of this licence, visit http://creativecommons.org/licenses/by/4.0/.

References

Allan DW (1966) Statistics of atomic frequency standards. Proc IEEE 54(2):221–230. https://doi.org/10.1109/PROC.1966.4634

Calliess D, Montenbruck O, Wermuth M, Reichinger H (2024) Long-term analysis of sentinel-6A orbit determination: insights from three years of flight data. Adv Space Res 74(7):3011–3027. https://doi.org/10.1016/j.asr.2024.06.043

Colombo O (1989) The dynamics of global positioning system orbits and the determination of precise ephemerides. J Geophys Res Atmos 94(B7):9167–9182. https://doi.org/10.1029/JB094iB07p09167

Dach R, Lutz S, Walser P, Fridez P (2015) Bernese GNSS software version 5.2. https://doi.org/10.7892/boris.72297

Dach R, Schaer S, Arnold D, Brockmann E, Kalarus MS, Lasser M, Stebler P, Jäggi A (2024) CODE final product series for the IGS. https://doi.org/10.48350/197025

Darugna F, Casotto S, Bardella M, Sciarratta M, Zoccarato P, Giordano P (2022) Sentinel-6A GPS and Galileo dual-frequency real-time reduced-dynamics P2OD. In: 10th workshop on satellite navigation technology (NAVITEC), https://doi.org/10.1109/NAVITEC53682.2022.9847561

Donlon CJ, Cullen R, Giulicchi L, Vuilleumier P, Francis CR, Kuschnerus M, Simpson W, Bouridah A, Caleno M, Bertoni R et al (2021) The Copernicus Sentinel-6 mission: Enhanced continuity of satellite sea level measurements from space. Remote Sens Environ 258(112):395. https://doi.org/10.1016/j.rse.2021.112395

Dormand J, Prince P (1980) A family of embedded Runge-Kutta formulae. J Comput Appl Math 6(1):19–26. https://doi.org/10.1016/0771-050X(80)90013-3

Eissfeller B, Pany T, Dötterböck D, Förstner R (2024) A comparative study of LEO-PNT systems and concepts. In: Proceedings of the ION 2024 Pacific PNT Meeting. pp 758–782. https://doi.org/10.33012/2024.19646

EU (2026) Copernicus data space ecosystem. https://dataspace.copernicus.eu/, accessed on 2026-08-17

Fernández J, Peter H, Fernández C, Berzosa J, Fernández M, Bao L, Ángel Muñoz M, Lara S, Terradillos E, Féménias P, Nogueira C (2024) The Copernicus POD Service. Adv Space Res 74(6):2615–2648. https://doi.org/10.1016/j.asr.2024.02.056

Giordano P, Zoccarato P, Walker R, Mandorlo G, Bouridah A, Crisci M (2018) ESA activities and plans for experimentation and exploitation of precise real-time on-board orbit determination (P2OD). In: NAVITEC 2018, 5 - 7 December 2018, ESA-ESTEC, ESA

Harris I, Priester W (1962) Time-dependent structure of the upper atmosphere, NASA TN-1443. Goddard Space Flight Center, MD

Hauschild A, Montenbruck O (2021) Precise real-time navigation of LEO satellites using GNSS broadcast ephemerides NAVIGATION: J Inst Navig 68(2):419–432. https://doi.org/10.1002/navi.416

Hauschild A, Montenbruck O, Steigenberger P, Martini I, Fernandez-Hernandez I (2022) Orbit determination of Sentinel-6A using the Galileo high accuracy service test signal. GPS Solut 26(4):120. https://doi.org/10.1007/s10291-022-01312-5

Iannucci PA, Humphreys TE (2022) Fused Low-Earth-Orbit GNSS. https://doi.org/10.1109/TAES.2022.3180000, arXiv:2009.12334

Johnston G, Riddell A, Hausler G (2017) The international GNSS service. In: Teunissen P, Montenbruck O (eds) Springer handbook of global navigation satellite systems, Springer, chap 33, pp 967–982, https://doi.org/10.1007/978-3-319-42928-1_33

Kozhaya S, Saroufim J, Kassas ZZM (2025) Unveiling Starlink for PNT. Navig J Inst Navig https://doi.org/10.33012/navi.685

Kunzi F, Montenbruck O (2022) Precise onboard time synchronization for LEO satellites. Navig J Inst Navig 69(3):531. https://doi.org/10.33012/navi.531

Kunzi F, Montenbruck O (2023) Precise disciplining of a chip-scale atomic clock using PPP with broadcast ephemerides. GPS Solutions 27(4):165. https://doi.org/10.1007/s10291-023-01496-4

Kunzi F, Braun B, Markgraf M, Montenbruck O (2023) A GNSS-synchronized satellite navigation payload for LEO PNT. In: Proceedings of the 36th international technical meeting of the satellite division of the institute of navigation (ION GNSS+ 2023), pp 1425–1435, https://doi.org/10.33012/2023.19322

Kunzi F, Braun B, Markgraf M, Pintor P, Bauerhin A (2026a) Orbit determination and time synchronization in real-time using Galileo HAS: The HAUT-S satellite payload. In: Proc. NAVITEC 2026

Kunzi F, Montenbruck O, Perazzetti F (2026) GNSS-based real-time orbit determination and prediction for LEO-PNT ephemeris generation. Adv Space Res 77(1):923–938. https://doi.org/10.1016/j.asr.2025.11.082

Kvas A, Brockmann JM, Krauss S, Schubert T, Gruber T, Meyer U, Mayer-Gürr T, Schuh WD, Jäggi A, Pail R (2020) GOCO06s-a satellite-only global gravity field model. Earth Syst Sci Data Discuss 2020:1–31. https://doi.org/10.5194/essd-13-99-2021

Le Priellec A, Giordano P, Cordero Limon M, Grec F, Prieto-Cerdeira R (2025) LEO-PNT end-to-end in-orbit demonstration: an ESA initiative to pave the way for a European GNSS constellation in LEO. In: Petrozzi-Ilstad M (ed) Small satellites systems and services symposium (4S 2024), International society for optics and photonics, SPIE, vol 13546, p 1354633, https://doi.org/10.1117/12.3062635

Levine WS (2019) The essentials of model predictive control. In: Raković SV, Levine WS (eds) Handbook of Model Predictive Control, Springer International Publishing, pp 3–27, https://doi.org/10.1007/978-3-319-77489-3_1

Loeb N, Su W, Doelling D, Wong T, Minnis P, Thomas S, Miller W (2018) Earth's top-of-atmosphere radiation budget. In: Liang S (ed) Comprehensive remote sensing, Elsevier, Oxford, pp 67–84, https://doi.org/10.1016/B978-0-12-409548-9.10367-7

Lombardi MA (2008) The use of GPS disciplined oscillators as primary frequency standards for calibration and metrology laboratories.

NCSLI Meas 3(3):56–65. https://doi.org/10.1080/19315775.2008.11721437
Lombardi MA (2016) Evaluating the frequency and time uncertainty of GPS disciplined oscillators and clocks. NCSLI Meas 11(3–4):30–44. https://doi.org/10.1080/19315775.2017.1316696
Lutwak R (2011) The SA45s chip-scale atomic clock—early production statistics. In: Proceedings of the 43rd annual precise time and time interval systems and applications meeting. pp 207–220
Lutwak R, Rashed A, Varghese M, Tepolt G, LeBlanc J, Mescher M, Serkland D, Geib K, Peake G, Römisch S (2007) The chip-scale atomic clock-prototype evaluation. In: Proceedings of the 39th annual precise time and time interval meeting, pp 269–290
Lyard FH, Allain DJ, Cancet M, Carrère L, Picot N (2021) FES2014 global ocean tide atlas: design and performance. Ocean Sci 17(3):615–649. https://doi.org/10.5194/os-17-615-2021
Mayer-Gürr T, Rieser D, Höck E, Brockmann JM, Schuh WD, Krasbutter I, Kusche J, Maier A, Krauss S, Hausleitner W, Baur O, Jäggi A, Meyer U, Prange L, Pail R, Fecher T, Gruber T (2012) The new combined satellite only model GOCO03s. International symposium on gravity, geoid and height systems. GGHS,
Microchip Technology Inc (2019) SA45s chip-scale atomic clock datasheet. https://ww1.microchip.com/downloads/aemDocuments/documents/FTD/ProductDocuments/Brochures/SA.45s-CSAC-Options-001-and-003-00002985.pdf, Accessed on 17 August 2026
Montenbruck O, Gill E (2000) Satellite orbits: models, methods, and applications. Springer, Berlin, Heidelberg
Montenbruck O, Hauschild A (2013) Code biases in multi-GNSS point positioning. In: Proceedings of the 2013 international technical meeting of the institute of navigation, pp 616–628
Montenbruck O, Ramos-Bosch P (2008) Precision real-time navigation of LEO satellites using global positioning system measurements. GPS Solut 12(3):187–198. https://doi.org/10.1007/s10291-007-0080-x
Montenbruck O, Steigenberger P (2022) BRD400DLR: DLR's merged multi-GNSS broadcast ephemeris product in RINEX 4.00 format. DLR/GSOC https://doi.org/10.57677/BRD400DLR
Montenbruck O, Steigenberger P (2025) The 2024 GPS accuracy improvement initiative. GPS Solut 29(1):33. https://doi.org/10.1007/s10291-024-01793-6
Montenbruck O, Garcia-Fernandez M, Williams J (2006) Performance comparison of semicodeless GPS receivers for LEO satellites. GPS Solut 10(4):249–261. https://doi.org/10.1007/s10291-006-0025-9
Montenbruck O, Schmid R, Mercier F, Steigenberger P, Noll C, Fatkulin R, Kogure S, Ganeshan AS (2015) GNSS satellite geometry and attitude models. Adv Space Res 56(6):1015–1029. https://doi.org/10.1016/j.asr.2015.06.019
Montenbruck O, Steigenberger P, Hauschild A (2018) Multi-GNSS signal-in-space range error assessment - Methodology and results. Adv Space Res 61(12):3020–3038. https://doi.org/10.1016/j.asr.2018.03.041
Montenbruck O, Hackel S, Wermuth M, Zangerl F (2021) Sentinel-6A precise orbit determination using a combined GPS/Galileo receiver. J Geod. https://doi.org/10.1007/s00190-021-01563-z
Montenbruck O, Kunzi F, Hauschild A (2022) Performance assessment of GNSS-based real-time navigation for the Sentinel-6 spacecraft. GPS Solut 26(1):12. https://doi.org/10.1007/s10291-021-01198-9
Montenbruck O, Kunzi F, Salgueiro FDO, Gini F, Limón MC (2025) GNSS-based synchronization and monitoring of LEO-PNT onboard time. Adv Space Res. https://doi.org/10.1016/j.asr.2025.09.047
Öhgren M, Bonnedal M, Ingvarson P (2011) GNSS antenna for precise orbit determination including S/C interference predictions. In: Proceedings of the 5th European conference on antennas and propagation (EUCAP). IEEE, pp 1990–1994
Oliveira Salgueiro D, Gini F, Kunzi F, Montenbruck F, Otten O, Mayer M, V, Limon C, Traiser M, B (2026) Performance assessment of onboard time-synchronization for LEO satellites. Proc. NAVITEC 2026
Picone JM, Hedin AE, Drob DP, Aikin AC (2002) NRLMSISE-00 empirical model of the atmosphere: Statistical comparisons and scientific issues. J Geophys Res Space Phys 107(A12):SIA 15–1–SIA 15–16, https://doi.org/10.1029/2002JA009430
Psiaki ML (2021) Navigation using carrier doppler shift from a LEO constellation: TRANSIT on steroids NAVIGATION: J Inst Navig 68(3):621–641. https://doi.org/10.1002/navi.438
Riley W, Howe D (2008) Handbook of Frequency Stability Analysis. https://tsapps.nist.gov/publication/get_pdf.cfm?pub_id=50505, accessed on 2026-08-17
Rizos C, Stolz A (1985) Force modelling for GPS satellite orbits. Proc. 1st Int. Sym. Precise Positioning with GPS, vol 1. Rockville, MD, pp 87–98
Tetewsky A, Ross J, Soltz A, Vaughn N, Anszperger J, O'Brien C, Graham D, Craig D, Lozow J (2009) Making sense of inter-signal corrections—accounting for gps satellite calibration parameters in legacy and modernized ionosphere correction algorithms. InsideGNSS, pp 37 –48a
Wang F, Gong X, Sang J, Zhang X (2015) A novel method for precise onboard real-time orbit determination with a standalone GPS receiver. Sensors 15(12):30,403–30,418, https://doi.org/10.3390/s151229805
Wu SC, Yunck TP, Thornton CL (1991) Reduced-dynamic technique for precise orbit determination of low Earth satellites. J Guid Control Dyn 14(1):24–30. https://doi.org/10.2514/3.20600

Publisher's Note Springer Nature remains neutral with regard to jurisdictional claims in published maps and institutional affiliations.

F. Kunzi is a member of the GNSS Technology and Navigation Group at DLR's German Space Operations Center (GSOC) and a PhD candidate at Technical University of Munich. He received his M.Sc. degree in Space Science and Technology from the University of Würzburg in 2018. His current work focuses on real-time orbit determination and time synchronization for LEO-PNT.

J. Holtkamp is a member of the GNSS Technology and Navigation Group at DLR's German Space Operations Center (GSOC). He received his M.Sc. degree in Earth Oriented Space Science and Technology from the Technical University of Munich (TUM) in 2024 and has since worked in the field of real-time orbit determination for LEO spacecraft.

O. Montenbruck is an honorary professor at Technische Universität München (TUM) and former head of the GNSS Technology and Navigation Group at DLR's German Space Operations Center. His research interests comprise space-borne GNSS receiver technology, GNSS-based autonomous navigation systems, precise orbit determination, multi-constellation GNSS, and LEO-PNT systems.